Cement and Concrete Research 41 (2011) 903–912

Contents lists available at ScienceDirect

Cement and Concrete Research

journal homepage: http://ees.elsevier.com/CEMCON/default.asp

Investigation on stress-crack opening relationship of engineered cementitious composites using inverse approach

Jun Zhang *, Xianchun Ju

Department of Civil Engineering, Tsinghua University, Beijing, 100084, PR China

ARTICLE INFO

Article history:
Received 21 September 2010
Accepted 21 April 2011

Keywords:
C, Tensile properties
E, Composites
E, Fiber reinforcement

ABSTRACT

The stress-crack opening relationship of engineered cementitious composites was determined with an inverse method. Four cement matrixes with water to cement ratio of 0.55, 0.45, 0.35, 0.25 and fiber contents of 0.5%, 1.0% in volume were selected to form different series of composites. The results show that the σ–w relationship of the cement matrix is instant strain softening after the cracking strength. After adding polyvinyl alcohol fibers, the stress-crack opening relationship of the composites changes to a double peak mode behavior as the crack bridging first decreases from cracking strength, then increases to the second peak. After that the tensile softening is displayed again with increase of crack opening. The cracking strength is governed by the cement matrix and the second peak stress is controlled by the fibers and fiber/matrix interface. The second peak is greatly increased with increase of fiber content. The second peak stress larger than the cracking strength means strain-hardening and multiple cracking performances can be expected under tension.

1. Introduction

Concrete is a typical brittle material where first cracking in tension is accompanied by immediate localization of deformation followed by decreasing load. In normal reinforced concrete structures, as the stress reaches the tensile strength of concrete under mechanical and/or environmental loads, a small number of widely spaced discrete cracks will form and the crack width quickly opens to a macroscopically visible level. The formation of widely opened cracks allows water and other chemical agents, such as deicing salt, to go through the cover layer to come into contact with the reinforcements. The durability of the concrete structure is then significantly affected. Many methods have been proposed to improve the durability of concrete structures in the past, but most focus on the transport properties of un-cracked concrete, with little attention paid to the control of cracks. To prevent the rapid penetration of water and corrosive chemicals through cracks, a fundamental approach to reduce the crack width in concrete during its service stage has to be developed [1].

In recent years, a class of high performance fiber reinforced cementitious composite, called Engineered Cementitious Composites (ECC), with an ultimate strength higher than the first cracking strength has been developed [2]. After first cracking, tensile load-carrying capacity continues to increase, resulting in strain-hardening accompanied by multiple cracking. For each individual crack, the crack width first increases steadily up to certain level and then stabilizes at a constant value. Further increase in strain capacity is capacity is achieved by the formation of additional cracks until the cracking reaches a saturated state with crack spacing limited by the stress transfer capability of the fibers. After that, a single crack localizes and the load slowly drops with increased deformation. Typically, strain localization occurs at a tensile strain of 2–4%, with crack spacing of 3–6 mm and crack width around 60 μm [2]. Typical tensile stress–strain curve and some photos of crack pattern under tension of such material are shown in Fig. 1 [3]. Cracks of such a small width will have little effect on the water permeability of the material [4]. With little degradation in transport properties under high deformation, the durability of the structure can be maintained. Due to the super mechanical and crack control performances, the conditions of the composite to achieve above performance are of great interest from the point of material design.

The design criterion for ECC has first been proposed by Li and Leung [5] and further developed in subsequent investigations [6–8]. The requirements for steady state crack propagation necessary for cementitious composite strain-hardening behavior, and the micromechanics of the stress-crack opening relationship (σ–w) combine to provide the guidelines for the tailoring of fiber, matrix and interface in order to attain strain-hardening with the minimum amount of fibers [6]. Steady state crack propagation means that a crack extends at constant ambient tensile stress, while maintaining a constant crack opening. This phenomenon occurs when the below condition is satisfied [6].

$$\frac{K_m^2}{E_m} \le \sigma_0 w_0 - \int_0^{w_0} \sigma(w)dw \quad (1)$$

* Corresponding author. Tel.: +86 10 62797422; fax: +86 1062797422.
E-mail address: junz@tsinghua.edu.cn (J. Zhang).

0008-8846/$ – see front matter © 2011 Elsevier Ltd. All rights reserved.
doi:10.1016/j.cemconres.2011.04.010

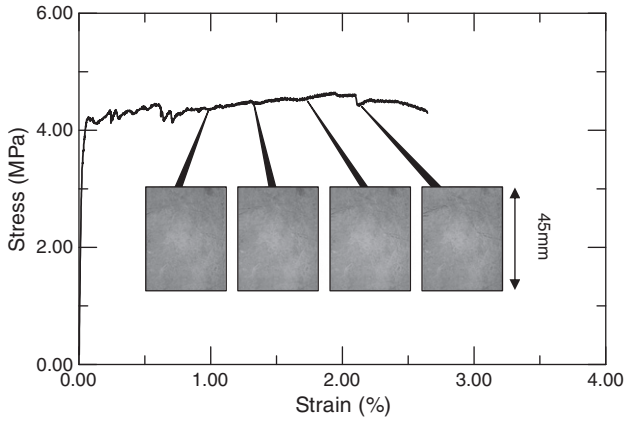

Fig. 1. Typical tensile stress–strain curve of ECC.

where K_m and E_m are fracture toughness and elastic modulus of the matrix, and σ_0 and w_0 are the peak crack bridging stress and the corresponded crack opening respectively. Clearly, successful design of an ECC composite with strain-hardening performance requires the tailoring of fiber, matrix and interface properties, which control the shape of $\sigma(w)$ curve and are therefore the dominant factors governing the value of the right hand side of Eq. (1). Thus, the stress-crack opening relationship (σ–w) of the composite and fracture toughness of matrix becomes the critical material parameters controlling the macro mechanical properties of the composites.

The direct tensile test is the most direct way to determine this relationship [9,10]. However, problems related to gripping, load eccentricity and the determination of exact crack location (for crack opening to be controlled) make the uniaxial tension test difficult to perform. To avoid the difficulties in the direct tension test, Li et al. [11] proposed a method based on J-integral technique to indirectly determine the stress-crack width relationship. Using notched beams with two different notch depths, experimentally determined load-displacement curves are used to derive the σ–w relationship. As the process involves the differentiation of experimental results, the accuracy of the derived σ–w relationship can be affected. Recently, methods such as the arthritis, rheumatism, and aging medical information system (ARAMIS) technology and 3D optical method with algorithms were used to deduct crack widths from deformation data of ECC with strain-hardening performance, from which the accurate crack width at various positions along a crack can be obtained [12,13]. These methods may overcome the difficulties in crack width measurement met in direct tensile tests on cementitious materials. Certainly, the specimen size effect on the results may still exist in these methods.

Inverse analysis methods have been developed to obtain the fracture parameters of concrete from the bending test recently [14,15]. In these analyses, the tensile strength is taken as the starting point of the stress-crack opening curve and is used as the criterion to check if the crack has started to propagate. However, the starting point of the σ–w curve should be the cracking strength of the material rather than the ultimate tensile strength [16]. In the case of cement paste or very high strength concrete the difference between them may be very small. For normal concrete materials, these two values are significantly different in both meaning and value. The cracking strength represents the bond strength between cement matrix and aggregate and the tensile strength is the maximum tensile stress that can be carried. From the theoretical point of view, and as verified by experimental investigations, the tensile strength can be higher than the cracking strength because the aggregates can provide a bridging stress beyond the applied stress when cracking first occurs. To check if a crack has started to propagate, the cracking strength should hence be used instead of the tensile strength. An inverse analysis method for the determination of σ–w relationship of cementitious material based on cracking strength criterion was developed by Zhang et al. [16].

In the present paper, the stress-crack opening relationship (σ–w) of ECCs is determined from three-point bending test by inverse analysis first. The cracking strength is used as cracking criterion in the inverse analysis. The influences of water to cementitious material ratio and fiber content on the shape of the σ–w curves are analyzed. Based on the σ–w relationship, the requirements for strain-hardening and multiple cracking for fiber reinforced cementitious composite are discussed.

2. Determination of σ–w relationship of ECC from bending test

2.1. Simulation of crack propagation in cement composite under bending load

Currently, there are two kinds of criteria that are normally used in the analysis of crack propagation in concrete. One is the strength criterion [17,18] and the other is the fracture toughness criterion [19,20]. The strength criterion is based on the assumption that the stress singularity at the crack tip is eliminated by the fictitious force in the fracture process zone around the crack tip. Thus, the principal tensile stress at the crack tip (σ_{tip}) during the crack propagation should be equal to the cracking strength of concrete, i.e.

$$\sigma_{tip} = \sigma_{fc} \tag{2}$$

The fracture toughness criterion assumes the stress singularity at the crack tip still exists and the fictitious force in the process zone reduces the fracture toughness at the crack tip. The total fracture toughness at crack tip (K_{tip}) is equal to the fracture toughness of cement matrix (K_m) and remains a constant during crack propagation, i.e.

$$K_{tip} = K_m \tag{3}$$

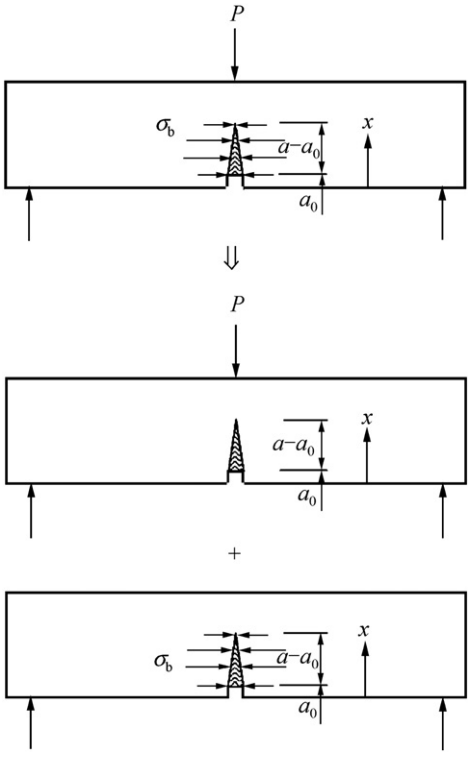

Fig. 2. Principle of superposition in cracking concrete beam under bending load and fictitious force.

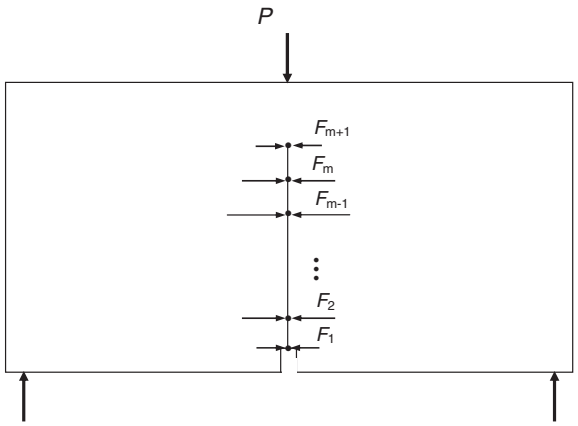

Fig. 3. Finite element nodes and fictitious force on node along the potential fracture line.

In the following, the cracking criterion will be used for obtaining the stress-crack opening relationship of ECCs.

Considering a central pre-notched concrete beam under three-point bending load (see Fig. 2), the direction of crack propagation should be perpendicular to the maximum principal stress. Therefore the crack propagation path in this load configuration can be predicted in advance, i.e. parallel to the load, from the notch tip upwards to the beam top. Here the fictitious crack tip is defined as the point where the principal tensile stress attains the cracking strength σ_{fc} and the crack opening at this point is equal to zero. The material in the process zone is still able to transfer stress which is governed by the crack opening displacement w. The relationship between the cohesive stress and the crack opening can be expressed by a multi-linear equation, i.e.:

$$\sigma_n = k_n w + \sigma_{0n} \quad for \quad w_{n-1} \le w \le w_n \ (n = 1, 2, \ldots, n_{max}) \tag{4}$$

where k_n is the slope for $w \in [w_{n-1},\ w_n]$. $\sigma_{01} = \sigma_{fc}$, $\sigma_{0n} = \sum_{1}^{n-1} [(k_i - k_{i+1}) w_i] + \sigma_{fc}$. Fig. 2 shows a cracked beam section with initial notch length a_0, crack length a and external load P. The fictitious bridging stress acting on the crack surface along the cracking section is $\sigma_b(w(x))$. According to the principle of superposition shown in Fig. 2, the crack opening along the crack length can be obtained by summing the contributions of external load and the bridging force, i.e.

$$w(x) = k_{pw}(x) P - B \int_0^a k_{fw}(x, y) \sigma_b(y) dy \quad for \quad 0 \le x < a \tag{5}$$

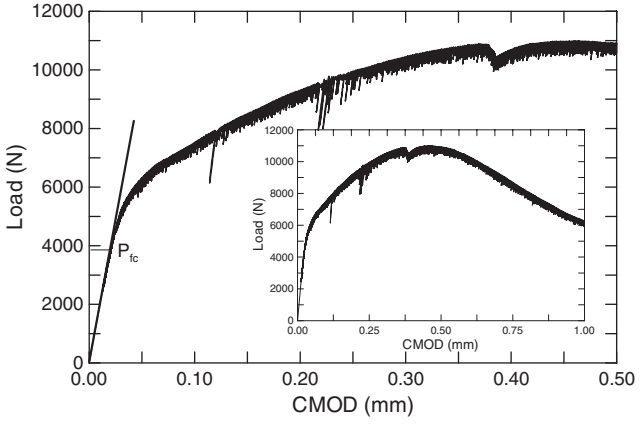

Fig. 4. Determination of cracking load from P–CMOD curves.

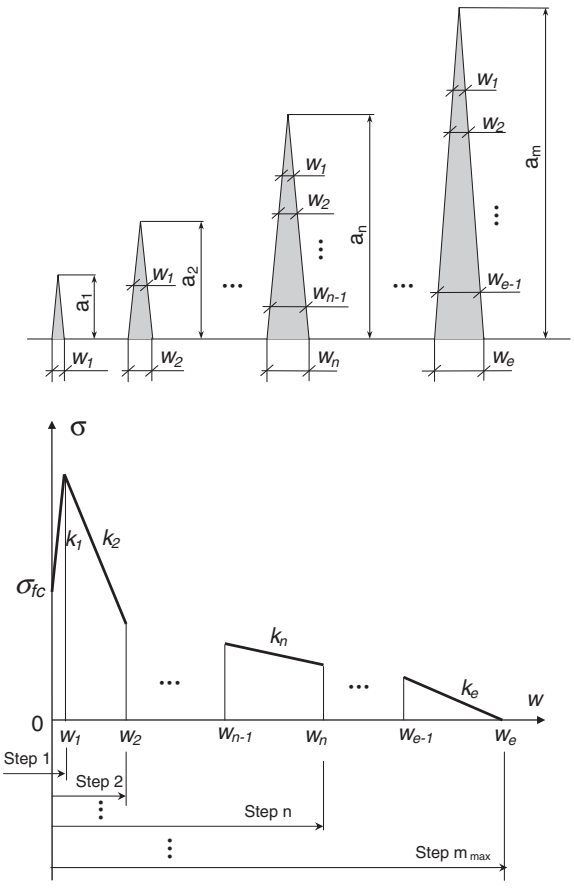

Fig. 5. Determination procedures of stress-crack opening relationship.

Similar, the stress at the crack tip can be obtained by

$$\sigma_{tip} = k_{p\sigma} P - B \int_0^a k_{f\sigma}(x, y) \sigma_b(y) dy \quad for \quad 0 \le x < a \tag{6}$$

As the equilibrium achieved, $\sigma_{tip} = \sigma_{fc}$. k_{pw}, k_{fw} and $k_{p\sigma}$, $k_{f\sigma}$ are the influencing factors of external load and fictitious force on the crack opening and crack tip stress respectively. Instead of solving the above equation by integration during iteration towards self-consistency to $w(x)$, the problem can be solved in the matrix form which can greatly enhance the computational procedures especially when many applied load levels need to be considered to improve the precision of the derived σ–w relation. With reference to the bending specimen shown in Fig. 3, the nodes are distributed along the

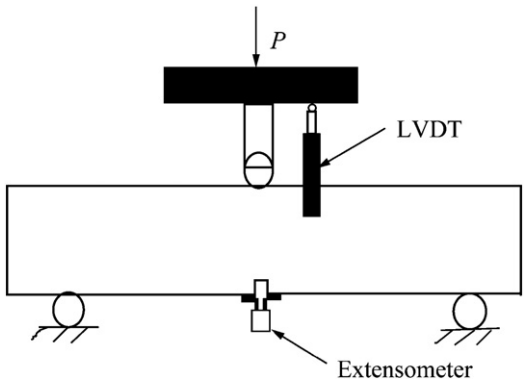

Fig. 6. Test set-up of bending test.

Table 1
Properties of the PVA fiber.

Density (g/cm3)	Tensile strength (MPa)	E (GPa)	Diameter (mm)	Length (mm)
1.2	1620	42.8	0.039	12

Table 2
Mix proportions of ECCs.

Mix no.	Cement	Water	Sand	Super plasticizer	Fiber (volume, %)		
1	1.0	0.55	0.8	0.010	1.0	0.5	0
2	1.0	0.45	0.8	0.012	1.0	0.5	0
3	1.0	0.35	0.3	0.012	1.0	0.5	0
4	1.0	0.25	0.3	0.022	1.0	0.5	0

potential fracture line. The closing stresses acting on the crack surface are replaced by nodal forces that are governed by the crack opening displacement according to the σ–w relationship of the material. When the cracking strength is achieved at the crack tip, the node is then split into two nodes and a pair of opposite nodal forces starts to act on these two nodes. The fictitious crack tip then moves to the next node. Let vector $w \equiv (w_1, w_2, w_3, \ldots w_m)$, $F \equiv (F_1, F_2, F_3, \ldots F_m)$, and assume the node number of the crack tip is $m+1$, then the Eqs. (5) and (6) can be expressed in index notation as:

$$w_i = k_{pw-i}P - \sum_{i=1}^{m} k_{fw-i}F_i \quad (i = 1,2,\ldots,m) \tag{7}$$

$$\sigma_{fc} = k_{p\sigma}P - \sum_{i=1}^{m} k_{f\sigma-i}F_i \quad (i = 1,2,\ldots,m) \tag{8}$$

F_i can be related with w_i by

$$F_i = (k_n w_i + \sigma_{oi})B\Delta l_i \quad (i = 1,2,\ldots,m) \tag{9}$$

where B is the specimen width and Δl_i is the calculating length at node i. Here Δl is the distance between two adjacent nodes. Generally $\Delta l_i = \Delta l$ except for $i=1$ when $\Delta l_i = 0.5\Delta l$. The influence factors for the opening at each node and crack tip principal stresses are obtained by a finite element analysis where the cracked beam shown in Fig. 3 is subjected to $m+1$ (P, F_1, …, F_{m+1}) different loading condition. For a given fictitious crack length a ($a = m\Delta l$), Eqs. (6), (7) and (8) turn into a linear algebraic system of $(2m+1)$ equations and $(2m+1)$ unknowns, i.e. $x \equiv (P, w_1, w_2, w_3, \ldots w_m, F_1, F_2, F_3, \ldots F_m)$. In addition, the crack mouth opening displacement w_0 can be related to P and F_i by

$$w_0 = k_{pw-0}P - \sum_{i=1}^{m} k_{fw-i}F_i \quad (i = 1,2,\ldots,m) \tag{10}$$

Thus, for a given crack length, a and stress-crack width relation, solving Eqs. (7), (8) and (9), the critical external load capacity P, fictitious force F_i and crack profile $w(x)$ can be obtained. The CMOD can then be calculated from Eq. (10).

2.2. Determination of cracking strength of matrix

To obtain the stress-crack width relationship, cracking strength σ_{fc} should be determined first. Cracking strength, defined as the stress level at which the initial crack starts to propagate, is determined directly from the results of three-point bending tests on pre-notched beams [16]. According to the elastic theory, for a given initial crack, the CMOD and external load (P) obeys a linear relationship before the initiation of cracking. After initial cracking, the linear relationship between P and CMOD does not exist any

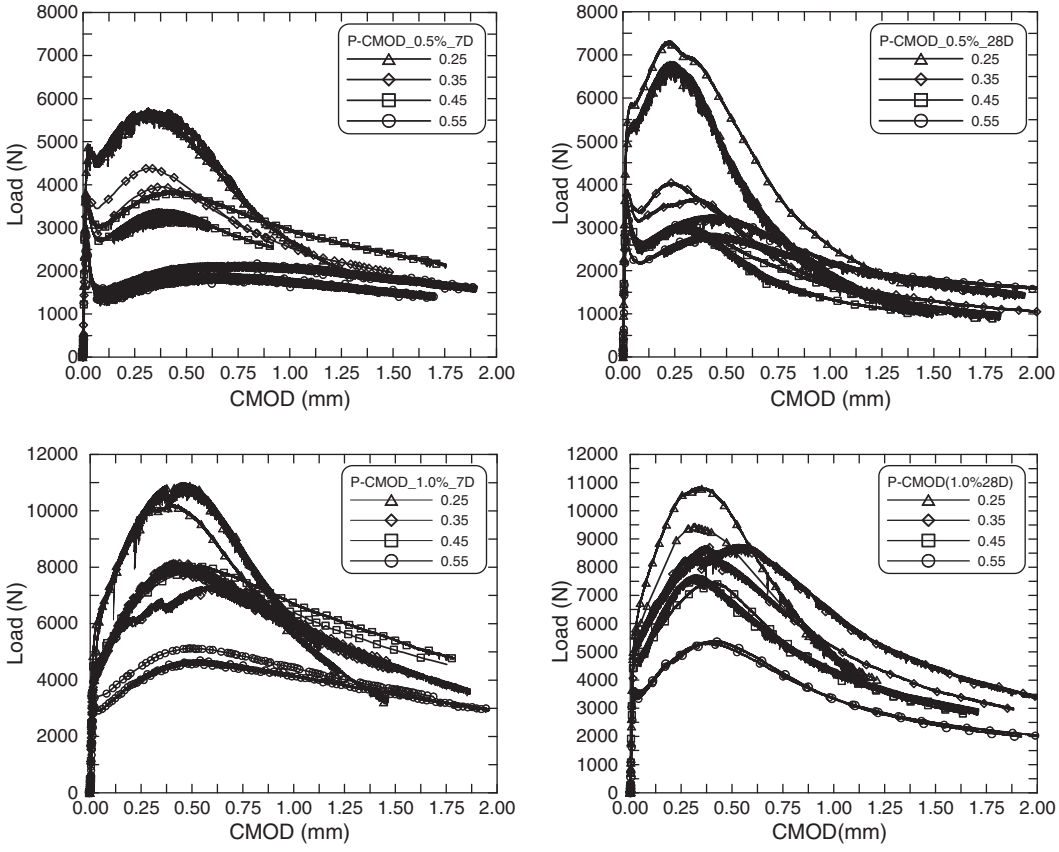

Fig. 7. Load–CMOD curves of different mixtures at 7 and 28 days.

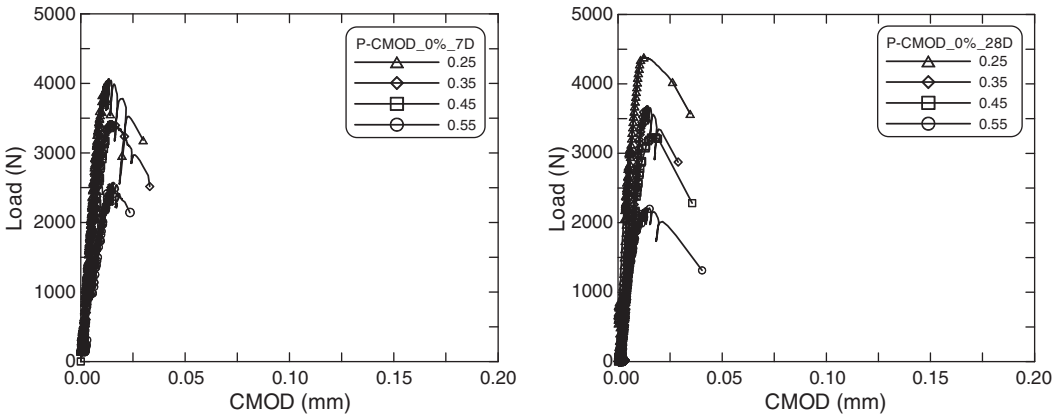

Fig. 8. Load–CMOD curves of matrixes at 7 and 28 days.

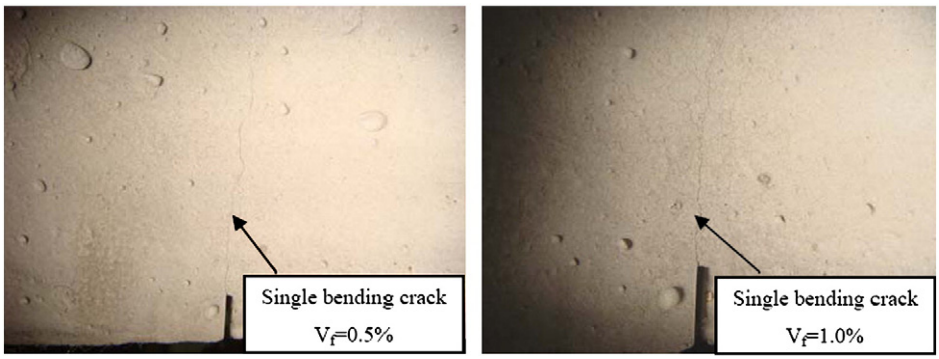

Fig. 9. Typical single crack patterns formed under bending load.

longer. Thus the cracking load, P_{fc} can be determined by the point where the P–CMOD curve deviates from the initial linear portion. This point is regarded as the transition point from the linear-elastic stage to the nonlinear-elastic stage, in which a fictitious crack starts to develop. Typical graphs illustrating the determination of cracking load from a three-point bending test result on a notched specimen is shown in Fig. 4. Based on the P_{fc} value, the corresponding cracking strength, σ_{fc}, is calculated from a finite element analysis. It should be noted that σ_{fc} obtained in this manner is dependent on element size, and this should be taken into account. In the present work, a mesh size with 1.25 mm in length was used. Further refine the mesh almost do not influence the principal tensile stress at the notch tip for a given load.

2.3. Inverse analysis process

In this section, the inverse method for determining stress-crack opening relationship from an experimental determined load–CMOD curve on pre-notched beam will be described. In the present study, a numerical procedure is implemented to simulate a loading process through stepwise increment of the fictitious crack length. The minimum crack length is Δl and may increase stepwise to the maximum value $m_{\max}\Delta l$. m_{max} is an integer which depends on the maximum node number. The number of nodes along the potential cracking line depends on the node density. The relationship between crack propagation stage and the required stress-crack width law in the calculation is shown in Fig. 5. In each crack propagation step, by minimizing the difference between the model calculated load and the experimental determined load, the stress-crack width relationship can be determined.

The detailed procedures can be summarized as follows:

Step 1 Determine cracking strength σ_{fc} from the load–CMOD curve.
Step 2 Let $a = a_1$, the inclination k_1 and corresponding crack opening w_1 can be determined by minimizing the difference between calculated and experimental load values at a given CMOD.
Step 3 Let $a = a_2$, the inclination k_2 and corresponded crack opening w_2 can be determined. Here the constitutive law determined by step 2 must be used for the zone where $w \le w_1$ (see Fig. 5).

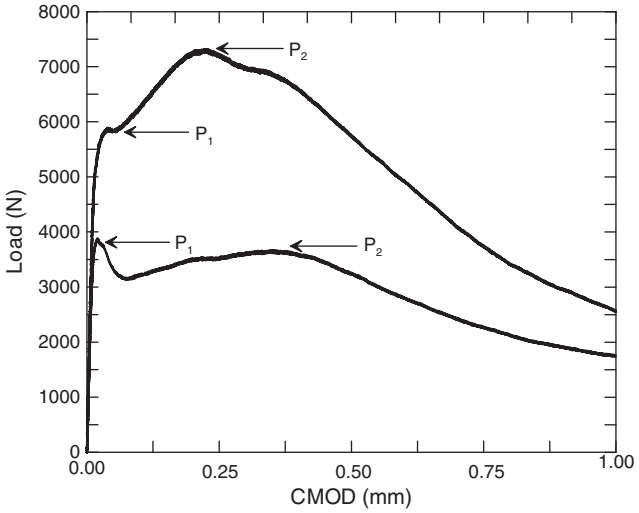

Fig. 10. Typical Load–CMOD curves of beams with different fiber contents.

Step 4 Let $a = a_3$, the inclination k_3 and corresponded crack opening w_3 can be determined. In this case, the constitutive law determined by step 2 and step 3 must be used for the zone $w \le w_1$ and $w_1 \le w \le w_2$.

By gradually increasing the crack length a up to $m_{max}\Delta l$, the whole stress-crack width relationship expressed as a multiple linear function as shown in Eq. (4) is obtained. The number of steps from step 2 to Step m_{max} depends on the accuracy requirement, calculation speed and number of nodes along the cracking line. In the present work, 16 steps were used to derive the stress-crack width relationship of ECCs.

3. Experimental program

In order to obtain the stress-crack opening relationship of ECCs, a simple three-point bending test with central pre-notched beam 400 mm × 100 mm × 100 mm in size is adopted. A standard Toni linear variable differential transducer (LVDT) is used for measuring the deflection. The crack mouth opening displacement (CMOD) is

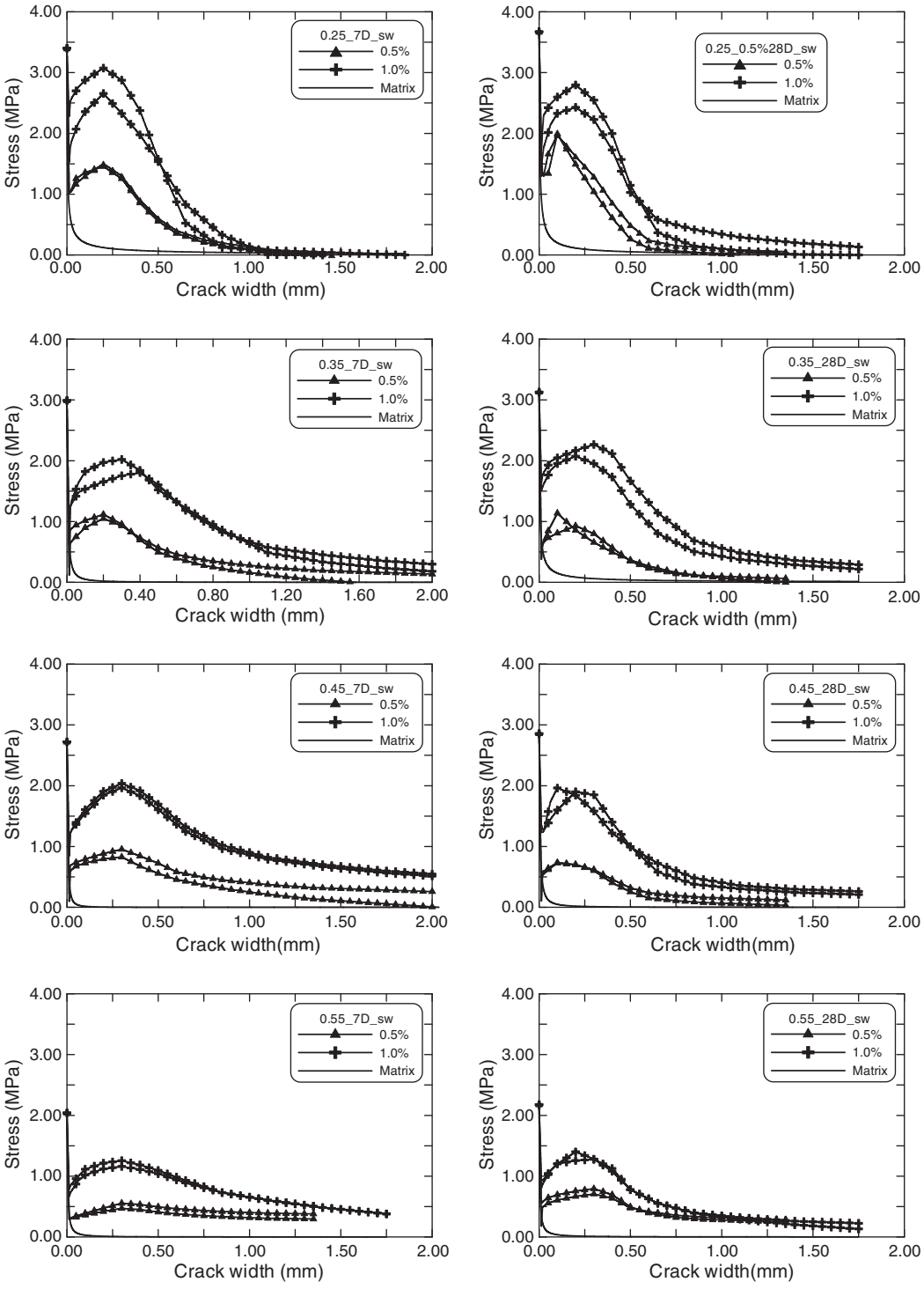

Fig. 11. Derived stress-crack opening (σ–w) relationship of all mixtures at 7 and 28 days.

measured by an extensometer with 10 mm gauge length mounted across the 10 mm deep and 3 mm wide notch. The test set-up and the geometry of the test specimen are shown in Fig. 6. The bending test is conducted at a prescribed deformation rate of 0.1 mm per minute using the signal from the LVDT as feedback. All tests are carried out on a Toni testing machine equipped for close-loop testing. The raw data consisted of time, load and displacement reading from load cell, LVDT and extensometer respectively. Data are recorded by the test machine and transferred to a computer for further processing.

The present investigation used new developed composited cement with low drying shrinkage characteristic and silica sand with average particle size of 0.1 mm to form the matrix [3,21]. Polyvinyl Alcohol fibers (PVA) supplied by Kuraray Company in Japan were used as reinforcement with the fiber properties listed in Table 1. To investigate the effect of the water to binder ratio (w/c) on the stress-crack opening relationship, four different w/c of 0.25, 0.35, 0.45, 0.55 and three different fiber content of 0, 0.5% and 1% in volume were used in the experiments. Here, it should be noted that in order to obtain a single crack under bending load, relative low fiber contents were used in the bending tests. Because high fiber content may lead to multiple cracking around the notch and this will destroy the basic assumptions used in the determination of stress-crack opening relationship from the bending test. The mixture proportions used in this study are listed in Table 2. The supperplasticizer was used to maintain a similar workability for all mixtures.

The mixing procedure of the composite material consists of the following steps.

(1) Matrix preparation: the matrix was prepared in a mortar mixer. First, the cementitious material and silica sand were mixed together for 2 min at low speed. Then water with superplasticizer (NF-5) and viscous agent (methyl cellulose) was gradually added, and mixing was continued for 2 min, resulted in a uniform fluid matrix. Within this period, the bottom of the mixing bowl was scraped manually to ensure that no solid materials stick to the bottom. After scraping, the matrix was mixed at a higher speed for 1 min before addition of fibers. (2) Addition of fibers: the fibers were gradually spread into the mixer by hand as the matrix was mixed at slow speed. The fibers must be added slowly to ensure proper distribution with no fibers bundled together. (3) Casting and curing: the composite material was carefully cast into the mold in two layers. First about half the material was placed. Then the mix was vibrated for 1–2 min to ensure that the material was well compacted. Then, the second half of the mold was filled with the composite in the same manner. After smoothing the surface, the specimens were covered with a polyethylene sheet to prevent moisture loss. After curing for 24 h at room temperature, the specimens were removed from their moulds and put into a curing room with temperature of 20 °C and a relative humidity above 90% for 7 and 28 days respectively before testing.

4. Results and discussions

4.1. Three-point bending test results

Typical bending test results in terms of Load–CMOD curves of the four series of cement composites with two different fiber contents are plotted in Fig. 7. The results of the reference beams without fiber addition are shown in Fig. 8. The typical single crack patterns formed under bending load are displayed in Fig. 9. From the results first we can see that the addition of PVA fiber can greatly improve the bending performance. Under three-point bending load, the cement matrix is brittle, with a sudden drop in resistance after the peak. With fibers added, the bending performance of beams is improved in both load-carrying capacity and ductility in terms of crack mouth opening displacement at peak load. Secondly, a similar pattern of the Load–CMOD curves of the pre-notched fiber reinforced beams can be found. From the Load–CMOD curve, the bending crack propagation of the pre-notched beam can be divided into two stages: (1) elastic stage with a constant stiffness (ΔP/ΔCMOD), up to the point of crack initiation when σ_{fc} is reached, the corresponding load is P_{fc}; (2) crack developing stage, with a pattern of load first increasing up to the first peak (P_1) then a small drop, followed by an increase up to the second peak (P_2). Typical test results showing above performance is displayed in Fig. 10. The magnitude relationship between P_1 and P_2 depends on the content of fiber and matrix strength (represented by the w/c ratio). As $V_f = 0.5\%$, for w/c = 0.25 and w/c = 0.35, $P_1 < P_2$ and for w/c = 0.35 and w/c = 0.45, $P_1 > P_2$. As $V_f = 1.0\%$ all beams behaves as $P_1 < P_2$. For different w/c ratio's, significant differences can be observed in terms of the maximum bending load and the stiffness in each stage. These differences are all related to its σ–w relationship. The σ–w relationships of all mixtures at 7 and 28 curing days are determined according to the procedures described in Section 2. The result presentation and further discussions on the effects of fiber content and matrix strength on the σ–w relationship are given in the following.

4.2. Stress-crack opening (σ–w) relationship of ECCs with low fiber content

Fig. 11 presents the solved σ–w curves of all mixtures listed in Table 2. The σ–w of the pure matrix is also shown in the figure. From these results, first we can see that the addition of PVA fibers can apparently enhance the crack bridging stress of the composite. The σ–w relationship of cement matrix shows significant tensile softening starting from cracking strength (σ_{fc}) immediately. After adding the PVA fibers, the σ–w relationship of the composite changes to double peak (σ_1 and σ_2) shape behaving as the crack bridging stress first decreases from cracking strength ($\sigma_1 = \sigma_{fc}$) to the lowest level, then increases to the second peak (σ_2). After that the tensile softening performance is displayed with increase of crack opening. This specific crack bridging performance with double peaks is more clearly displayed in Fig. 12. Such double peak behavior is the results of the combination of tensile softening of matrix bridging and tensile hardening of fiber bridging respectively. The first peak (σ_1) is governed by the matrix and the second peak (σ_2) is controlled by the PVA fibers as well as the fiber/matrix interface. Apparently, σ_2 increases with fiber content and matrix strength, as shown in Fig. 11. In addition, from the results we can observe that the second peak stress of the composite with fiber content of 1.0% is almost two

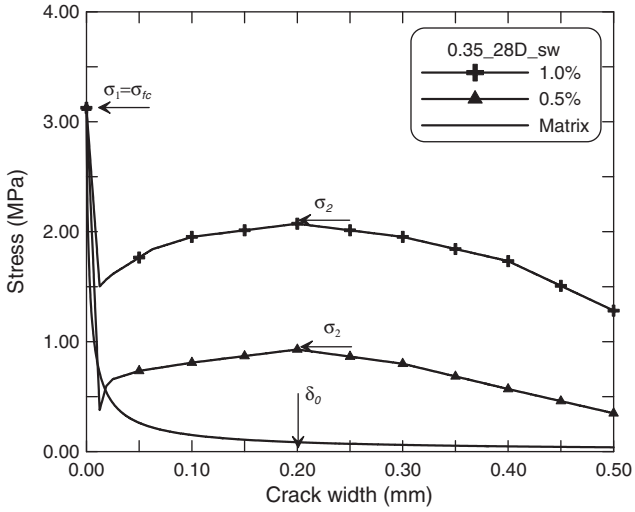

Fig. 12. Typical stress-crack opening (σ–w) relationship with single and double peak characteristics.

times higher than that of the composite with fiber content of 0.5%. Therefore, it may be concluded that for a given matrix the fiber bridging is proportional to the fiber content, as predicted by a theoretical model presented in [22].

4.3. Stress-crack opening relationship (σ–w) of ECC with high fiber content

In order to investigate the conditions to achieve strain-hardening and multiple cracking of ECCs, the σ–w relationship of the materials with high fiber content are studied by subtracting the contribution of matrix from the total crack bridging. The complete crack bridging (σ_t) in fiber reinforced cementitious composite is composed of matrix bridging (σ_m) and fiber bridging (σ_f), i.e.:

$$\sigma_t = \sigma_m + \sigma_f \tag{11}$$

Thus, the fiber bridging can be obtained by:

$$\sigma_f = \sigma_t - \sigma_m \tag{12}$$

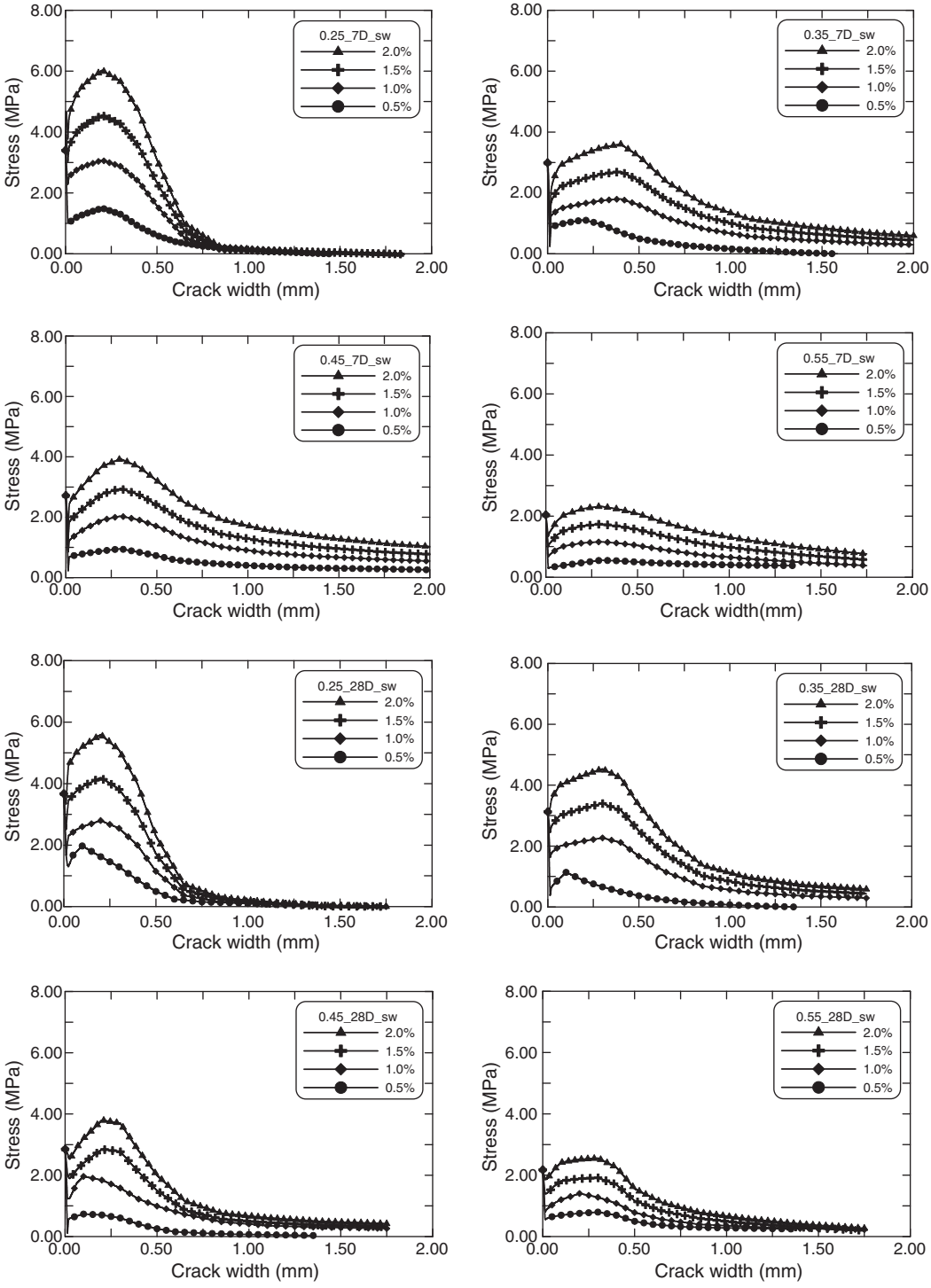

Fig. 13. Derived stress-crack opening (σ–w) relationship for high fiber content at 7 and 28 days.

The previous theoretical study [22] and present results (see Fig. 11) have shown that the fiber bridging σ_f is proportional to fiber content (V_f), and it can be expressed as:

$$\sigma_f = V_f \sigma_{f1} \tag{13}$$

where σ_{f1} is the fiber bridging stress of unit fiber volume content. Thus, as long as the fiber bridging stress with a given fiber content is known, the fiber bridging stress with any other content of fiber can be obtained by multiplying a factor related with fiber content. Here it is assumed that the fiber/matrix interfacial parameters are not influenced by fiber concentration in matrix. This assumption is reasonable for fiber content below 3% by volume in ECC [23]. Fig. 13 shows the deduced σ–w relationships of all ECC mixtures with fiber content up to 2% for curing age of 7 and 28 days. A typical σ–w relationships displaying the double peak characteristic more clearly is presented in Fig. 14. From the results, first we can observe that the second peak in the σ–w curves is significantly increased with fiber content. In some cases, the second peak σ_2 is already higher than the first peak σ_1. This means strain-hardening and multiple cracking performances may be obtained in such composite. That is because from Eq. (1), the right hand side is larger than zero only as $\sigma_2 > \sigma_1$. Therefore, the steady state matrix cracking requirement [5–7] is satisfied. Then if the Eq. (1) is satisfied also, strain-hardening and multiple matrix cracking behaviors can be expected. The relationship between σ_2/σ_1 and w/c of the composites with different fiber content at 7 and 28 days are displayed in Fig. 15(a) and (b) respectively. Clearly, the possible strain-hardening and multiple cracking performances can be achieved for the composites with fiber content above 1.5% in volume. The experimental results showed that the composites with fiber content of 1.7% behave apparent strain-hardening and multiple matrix cracking performances [3]. As $\sigma_2 < \sigma_1$, the tensile softening and single matrix cracking performances can be expected even the matrix is reinforced with fibers. It should be noted that although Fig. 15 shows that the ratio of σ_2/σ_1 is increased with decrease of w/c, for a given fiber content, the strain-hardening and multiple matrix cracking behaviors may be enhanced with decrease in w/c. The value of left hand side in Eq. (1) is also a controlling parameter for such performance and it is known that fracture toughness of matrix (K_m) is increased with decrease of w/c [24,25].

It should be pointed out that the stress-crack opening (σ–w) relationship of engineered cementitious composites (ECC) present in this paper is based on an indirect method. As a methodology to derive the stress-crack width relation, validation of the method is essential.

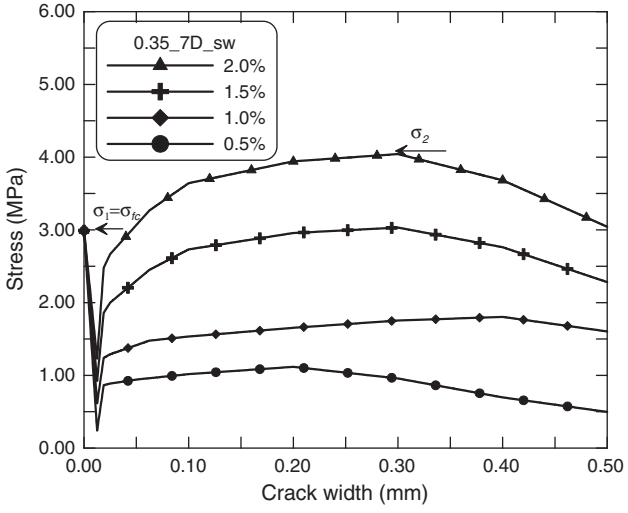

Fig. 14. Detailed double peak shape stress-crack opening relationship of ECCs.

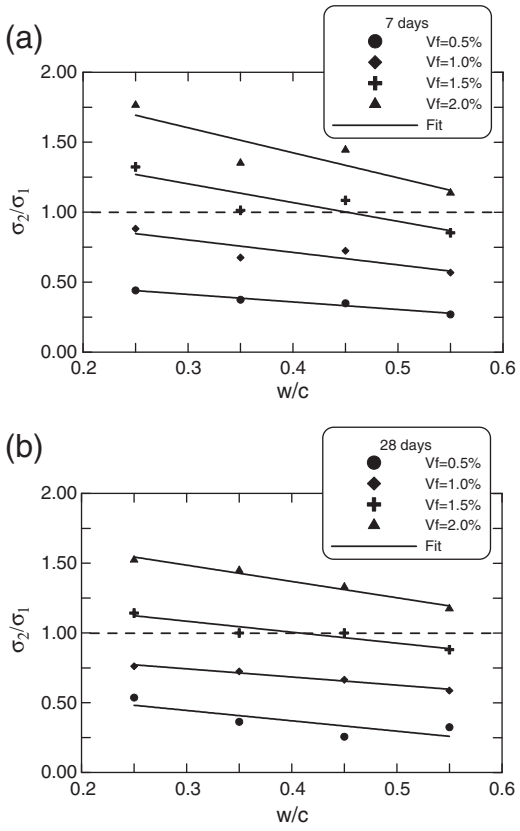

Fig. 15. Relationship between σ_2/σ_1 and w/c, (a) 7 days and (b) 28 days.

Additional work is needed in the future to compare the present results with the direct tensile data, in which the recent developed test methods [12,13] focusing on overcoming the difficulties met in the exact crack width measurement may prefer to be used.

5. Conclusions

In this paper the stress-crack opening (σ–w) relationship of engineered cementitious composites (ECC) is determined by an inverse method from a deformation controlled three-point bending test. The method relies on the fictitious crack model and is applicable with either the cracking strength criterion or fracture toughness criterion. The advantage of the present method is that only a simple testing machine with displacement control is necessary for the bending test, while the uniaxial tensile test for determining the σ–w relationship requires a much more sophisticated testing system.

Four cement matrixes with water to cementitious material ratio of 0.55, 0.45, 0.35, 0.25 and four fiber contents of 0.5%, 1.0%, 1.5%, and 2% in volume were selected to form different series of composites. The results show that the σ–w relationship of cement matrix is tensile softening starting from cracking strength (σ_{fc}) immediately. With PVA fibers added, the σ–w relationship of the composite changes to an double peak (σ_1 and σ_2) shape behaving as the crack bridging stress first decreases from cracking strength ($\sigma_1 = \sigma_{fc}$) to the lowest level, then increases to the second peak (σ_2). After that the tensile softening is displayed with increase of crack opening. The double peak behavior is the result of the combination of tensile softening of matrix bridging and tensile hardening of fiber bridging. The first peak (σ_1) is controlled by the matrix and the second peak (σ_2) is controlled by fibers and fiber/matrix interface. The second peak is increased with fiber content. $\sigma_2 > \sigma_1$ means strain-hardening and multiple cracking performance may be obtained in the composite. From present study, the possible strain-hardening and multiple cracking performances

can be achieved for the composite with fiber content above 1.5% in volume. As $\sigma_2 < \sigma_1$, the tensile softening and single matrix cracking performances can be expected even the matrix is reinforced with fibers.

Acknowledgements

Support from the National Science Foundation of China (No. 50878119) to Tsinghua University is gratefully acknowledged.

References

[1] M.D. Lepech, V.C. Li, Long term durability performance of engineered cementitious composites, International Journal for Restoration of Buildings and Monuments 12 (2) (2006) 119–132.
[2] V.C. Li, Advances in ECC Research, ACI Special Publication on Concrete: Material Science to Applications, SP 206-23 (2002) 373–400.
[3] J. Zhang, C.X. Gong, M.H. Zhang, Z.L. Guo, Engineered cementitious composite with characteristic of low drying shrinkage, Cement and Concrete Research 39 (4) (2009) 303–312.
[4] K. Wang, K. Wang, D. Jansen, S. Shah, A. Karr, Permeability study of cracked concrete, Cement and Concrete Research 27 (1997) 381–393.
[5] V.C. Li, C.K.Y. Leung, Steady state and multiple cracking of short random fiber composites, ASCE J. of Engineering Mechanics 118 (1992) 2246–2264.
[6] V.C. Li, From micromechanics to structural engineering — the design of cementitous composites for civil engineering applications, JSCE J. of Strutural Mechanics and Earthquake Engineering 10 (1993) 37–48.
[7] C.K.Y. Leung, Design criteria for pseudo-ductile fiber composites, ASCE J. of Engineering Mechanics 122 (1996) 10–18.
[8] T. Kanda, V.C. Li, A new micromechanics design theory for pseudo strain hardening cementitious composite, ASCE J. of Engineering Mechanics 125 (1999) 373–381.
[9] P.-E. Petersson, Crack growth and development of fracture zones in plain concrete and similar materials, Report TVBM-1006, Division of Building Materials, Lund Institute of Technology, 1981.
[10] Y.J. Wang, V.C. Li, S. Backer, Experimental determination of tensile behaviour of fibre reinforced concrete, ACI Materials Journal 87 (1990) 461–468.
[11] V.C. Li, C.M. Chan, C.K.Y. Leung, Experimental determination of the tension-softening relations for cementitious composites, Cement and Concrete Research 17 (1987) 441–452.
[12] V.Z. Gpag, F.H. Wittmann (Eds.), Durability of Strain-Hardening Fibre-Reinforced Cement-Based Composites (SHCC), State-of-the-Art Report, Rilem TC 208 HFC, SC 2, Springer Publishers, ISBN: 978-94-007-0337-7, 2011.
[13] C.J. Adendorff, W.P. Boshoff, G.P.A.G. van Zijl, Crack characterization in SHCC: towards durability assessment, Advances in Cement-based Materials: Proceedings International Conference on Advanced Concrete Materials, 17–19 November 2009, Stellenbosch, South Africa, 2010, pp. 215–221.
[14] Y. Kitsutaka, Fracture parameters by polylinear tension-softening analysis, Journal of Engineering Mechanics 123 (1997) 444–450.
[15] P. Nanakorn, H. Horii, Back analysis of tension-softening relationship of concrete, J. Materials, Conc. Struct., Pavements, JSCE 32 (544) (1996) 265–275.
[16] J. Zhang, C. K.Y. Leung, S. Xu, Evaluation of fracture parameters of concrete from bending test, Materials and Structures 43 (6) (2010) 857–874.
[17] J. Zhang, H. Stang, Application of stress crack width relationship in predicting the flexural behavior of fiber reinforced concrete, Cement and Concrete Research 28 (1998) 439–452.
[18] A. Carpinteri, B. Chiaia, G. Ferro, Scale dependence of tensile strength of concrete specimens: a multifractal approach, Magazine of Concrete Research 50 (1998) 237–246.
[19] V.C. Li, Matsumoto, T, Fatigue crack growth analysis of fiber reinforced concrete with effect of interfacial bond degradation, Cement and Concrete Composites 20 (5) (1998) 339–351.
[20] J. Zhang, V.C. Li, Simulation of crack propagation in fiber reinforced concrete by fracture mechanics, Cement and Concrete Research 34 (2004) 333–339.
[21] J. Zhang, C. Gong, Gong, Z. Guo, X. Ju, Mechanical performance of low shrinkage engineered cementitious composite in tension and compression, Journal of Composite Materials 43 (22) (2009) 2571–2584.
[22] V.C. Li, H. Stang, H. Krenchel, Micromechanics of crack bridging in fibre reinforced concrete, Materials and Structures 26 (1993) 486–494.
[23] V.C. Li, C. Wu, S. Wang, A. Ogawa, T. Saito, Interface tailoring for strain-hardening PVA–ECC, ACI Materials Journal 99 (5) (2002) 463–472.
[24] J. Zhang, C.K.Y. Leung, Y. Gao, Simulation of crack propagation of fiber reinforced cementitious composite with fracture mechanics model, Proceedings of the 7th International Conference on Fracture Mechanics of Concrete and Concrete Structures, pp.1401–1410, Jeju, Korea, 2010.
[25] V.C. Li, D.K. Mishra, H.C. Wu, Matrix design for pseudo strain-hardening fiber reinforced cementitious composites, Materials and Structures 28 (183) (1995) 586–595.